1-11-2016

Characterization of RNA Helicase CshA and Its Role in Protecting mRNAs and Small RNAs of Staphylococcus aureus Strain Newman

Samin Kim
Dartmouth College

Anna-Rita Corvaglia
Geneva University Hospital

Stefano Léo
Geneva University Hospital

Ambrose Cheung
Dartmouth College

Patrice Francois
Geneva University Hospital

AMERICAN SOCIETY FOR MICROBIOLOGY | Infection and Immunity

Characterization of RNA Helicase CshA and Its Role in Protecting mRNAs and Small RNAs of *Staphylococcus aureus* Strain Newman

Samin Kim,[a] Anna-Rita Corvaglia,[b] Stefano Léo,[b] Ambrose Cheung,[a] Patrice Francois[b]

Department of Microbiology and Immunology, Geisel School of Medicine at Dartmouth, Hanover, New Hampshire, USA[a]; Genomic Research Lab, Services of Infectious Diseases, Geneva University Hospital, Geneva, Switzerland[b]

The toxin $MazF_{sa}$ in *Staphylococcus aureus* is a sequence-specific endoribonuclease that cleaves the majority of the mRNAs *in vivo* but spares many essential mRNAs (e.g., *secY* mRNA) and, surprisingly, an mRNA encoding a regulatory protein (i.e., *sarA* mRNA). We hypothesize that some mRNAs may be protected by RNA-binding protein(s) from degradation by $MazF_{sa}$. Using heparin-Sepharose-enriched fractions that hybridized to *sarA* mRNA on Northwestern blots, we identified among multiple proteins the DEAD box RNA helicase CshA (NWMN_1985 or SA1885) by mass spectroscopy. Purified CshA exhibits typical RNA helicase activities, as exemplified by RNA-dependent ATPase activity and unwinding of the DNA-RNA duplex. A severe growth defect was observed in the *cshA* mutant compared with the parent when grown at 25°C but not at 37°C. Activation of $MazF_{sa}$ in the *cshA* mutant resulted in lower CFU per milliliter accompanied by a precipitous drop in viability (~40%) compared to those of the parent and complemented strains. NanoString analysis reveals diminished expression of a small number of mRNAs and 22 small RNAs (sRNAs) in the *cshA* mutant versus the parent upon $MazF_{sa}$ induction, thus implying protection of these RNAs by CshA. In the case of the sRNA teg049 within the *sarA* locus, we showed that the protective effect was likely due to transcript stability as revealed by reduced half-life in the *cshA* mutant versus the parent. Accordingly, CshA likely stabilizes selective mRNAs and sRNAs *in vivo* and as a result enhances *S. aureus* survival upon $MazF_{sa}$ induction during stress.

Discovered first as "addiction modules" in plasmids (1, 2), toxin-antitoxin (TA) systems have subsequently been found in the chromosomes of many pathogenic and nonpathogenic bacteria and *Archaea* (3–8). There are three types of TA systems, including RNA-RNA and protein-RNA systems (types I and III, respectively) and protein-protein systems (type II) (9). Chromosome-borne type II TA modules (9) are ubiquitous, with the small labile antitoxin binding the stable toxin to form an inert complex (5, 8). Upon stress (e.g., antibiotic, oxidation, or thymidine, or amino acid starvation) (10–15), the labile antitoxin will be degraded by ClpP in complex with specific adaptors (16, 17), thus unleashing the toxin to act on its target, which can be mRNA or other targets in the transcription/translation machinery (5). Additionally, there is accumulating evidence that TA modules may have an important role in stress physiology and quality control of gene expression by reducing production of proteins not essential to bacterial survival (5).

Salmonella enterica serovar Typhimurium (18) and *Mycobacterium tuberculosis* (19) have at least 11 and 88 type II TA modules, respectively, some of which are conserved in other pathogenic bacteria but absent from nonpathogenic species, suggesting that TA modules are critical to the virulence of these strains. In fact, the toxin-antitoxin genes *sehAB* in *S.* Typhimurium play a critical role in survival inside host cells (18).

In *Escherichia coli*, the best-studied TA module is MazEF. The MazF toxin in *E. coli* is an endoribonuclease, which preferentially cleaves mRNA between A and C residues at the ACA sequence in a ribosome-independent manner (20). Similar to what has been found in *E. coli*, the $MazF_{sa}$ toxin in *S. aureus* is also an endoribonuclease that cleaves sequence-specific mRNA, particularly at the VUUV′ sites, where V and V′ are A, C, and G but not U, both *in vivo* and *in vitro* (21, 22). As expected, the toxicity of $MazF_{sa}$ can be neutralized by coexpression with the antitoxin $MazE_{sa}$. Intriguingly, induction of the toxin $MazF_{sa}$ induces growth arrest, but the majority of the *S. aureus* cells remain viable, as indicated by Syto 9 staining (22). Follow-up studies disclosed that the effect of $MazF_{sa}$ on mRNA is selective, cleaving many mRNAs, including those of virulence genes (e.g., *agrA*, *hla*, and *spa*) but sparing housekeeping mRNAs such as *gyrB* and, surprisingly, the *sarA* mRNA, which encodes a regulatory protein (SarA) that controls the expression of toxins and cell wall proteins essential to virulence (22). Additional analysis indicated this "protective effect" is likely due to RNA-binding protein(s) (22). In this study, we conducted Northwestern blotting to show that the *sarA* mRNA hybridized with several protein bands eluted from a heparin-Sepharose column. Among them is an ~55-kDa protein that has been identified to be the DEAD box RNA helicase CshA. The *S. aureus cshA* mutant exhibited lower survival and viability than the parent upon $MazF_{sa}$ activation. Contrary to what has been ascribed to CshA as part of the degradosome to degrade mRNAs, we discovered that the expression of a number of mRNAs, many with important housekeeping functions, and ~22 small RNAs (sRNAs) was decreased in the *cshA* mutant versus the parent upon $MazF_{sa}$ activation. Further analysis of an sRNA called teg049—previously shown to modulate the *sarA* transcript level (23)—revealed that the half-life

Received 24 August 2015 **Returned for modification** 10 October 2015
Accepted 3 January 2016

Accepted manuscript posted online 11 January 2016

Citation Kim S, Corvaglia A-R, Léo S, Cheung A, Francois P. 2016. Characterization of RNA helicase CshA and its role in protecting mRNAs and small RNAs of *Staphylococcus aureus* strain Newman. Infect Immun 84:833–844. doi:10.1128/IAI.01042-15.

Editor: A. Camilli

Address correspondence to Ambrose Cheung, Ambrose.Cheung@dartmouth.edu.

TABLE 1 Strains and plasmids used in this study

Strain or plasmid	Genotype or characteristic(s)	Reference or source
Strains		
S. aureus		
RN4220	Mutagenized strain 8325-4 that accepts foreign DNA	25
Newman	Isolated from human infection in 1952	26
ALC6094	Newman with an IPTG-inducible T7 polymerase gene at *geh* locus	21
ALC6096	ALC6094 containing pG164::$mazF_{sa}$	21
ALC7201	ALC6094 Δ*cshA*::*kan*	23
ALC7214	ALC7201 with pG164::$mazF_{sa}$	This study
ALC7252	ALC7201 complement	25
ALC7273	ALC7252 with pG164::$mazF_{sa}$	This study
E. coli		
DH5α	F^- *endA1* ϕ80*lacZ*ΔM15 Δ(*lacZYA-argF*)*U169 recA1 hsdR17* (r_K^- m_K^+) *phoA supE44* λ^- *thi-1 gyrA96 relA1*	
BL21(DE3)(pLysS)	F^- *ompT hsdSB*(r_B^- m_B^-) *gal dcm*(DE3)(pLysS) (Cam^r)	
Rosetta(DE3)(pLysS)	F^- *ompT hsdSB*(r_B^- m_B^-) *gal dcm* (DE3)(pLysSRARE) (Cam^r)	
Plasmids		
pET15b	Ap^r, p_{T7lac}, His_6 coding sequence (5′), thrombin cleavage site	Novagen
pET22b(+)	Ap^r, p_{T7lac}, His_6 coding sequence (3′)	Novagen
pET28a(+)	Kan^r, His_6 coding sequence (5′ and 3′), thrombin cleavage site	Novagen
pMAD	*E. coli-S. aureus* shuttle vector containing temp-sensitive origin of replication, *bgaB* Erm^r Ap^r	51

of teg049 was reduced in a *cshA* mutant compared with the parent and complemented mutant. Collectively, these data suggest that CshA likely confers cell survival by offering protection to selective mRNA and a good number of sRNAs.

MATERIALS AND METHODS

Bacterial strains, plasmids, and culture media. The bacterial strains and plasmids used in this study are listed in Table 1. The *S. aureus* strain Newman (24) and its derivatives and strain RN4220 (25) were grown at either 37 or 25°C in tryptic soy broth (TSB) or agar (TSA). *E. coli* strains were grown in LB broth or agar. The following antibiotics were used when appropriate: erythromycin (2.5 μg/ml), chloramphenicol (10 μg/ml), tetracycline (2.5 μg/ml), rifampin (200 μg/ml), and kanamycin (50 μg/ml) for *S. aureus* strains and ampicillin (100 μg/ml) and kanamycin (100 μg/ml) for *E. coli* strains.

DNA manipulation and transformation. Standard procedures for DNA manipulations were used for cloning (26). Restriction endonucleases and DNA-modifying enzymes were purchased from New England BioLabs (NEB). *E. coli* and *S. aureus* plasmids were isolated with the QIA Prep Spin miniprep kit (Qiagen). Transformations of *E. coli* and *S. aureus* cells were carried out using MicroPulser (Bio-Rad). Recombinant plasmids obtained from *E. coli* were first transformed to *S. aureus* strain RN4220 for proper DNA methylation to reduce restriction barriers (22). The plasmids purified from RN4220 were then electroporated into *S. aureus* ALC6094, a derivative of strain Newman carrying the T7 RNA polymerase gene in the *geh* locus (21).

Preparation of the *sarA* mRNA probe. To obtain *sarA* mRNA, pET14b-*sarA* (1 μg) (22) was linearized with BamHI, incubated with components of the T7 Mega transcription kit (Ambion) for 2 h, and further treated with DNase I for 15 min at 37°C. The *sarA* transcript (5 μg) was dephosphorylated with 10 U of Antarctic phosphatase (NEB) and then radiolabeled with [γ-^{32}P]ATP at 37°C for 30 min in a 25-μl reaction volume using 4 U of T4 polynucleotide kinase (Invitrogen). Unincorporated nucleotides were removed using the RNeasy MinElute cleanup kit (Qiagen).

Expression of $MazF_{sa}$ in *E. coli* and *S. aureus*. Expression and purification of $MazF_{sa}$ from *E. coli* BL21 were performed as previously described by Fu et al. (22).

For ectopic expression of $MazF_{sa}$ in *S. aureus*, ALC6096 cells with shuttle plasmid pG164::$mazF_{sa}$ were grown overnight at 37°C, inoculated into fresh TSB medium containing 10 μg/ml chloramphenicol, grown until they reached an optical density at 650 nm of (OD_{650}) of ~0.4, and induced with 1 mM IPTG (isopropyl-β-D-thiogalactopyranoside). The control contains no IPTG. After growing for an additional 80 min, cells were harvested, resuspended in buffer A (20 mM Tris-HCl [pH 8.0], 50 mM NaCl, 10 mM $MgCl_2$, 1 mM dithiothreitol [DTT], 0.5 mM EDTA, 5% glycerol), and homogenized with a reciprocal shaker (Biospec, Inc.) in the presence of 0.1-mm glass/zirconia beads as described previously (17). After centrifugation (20,200 × *g* for 30 min), supernatants were loaded onto a 5-ml heparin-Sepharose column (GE-Amersham) and eluted with a linear NaCl gradient of 0.02 to 1 M at a flow rate of 1 ml/1 min, collecting over 50 fractions (27).

Northwestern blots of cellular fractions with a *sarA* mRNA probe. Proteins in the collected fractions were precipitated by 10% trichloroacetic acid (TCA), centrifuged at 20,200 × *g* for 15 min, washed with cold acetone, dissolved in loading buffer, resolved in 15% sodium dodecyl sulfate (SDS)-polyacrylamide gel electrophoresis (PAGE), blotted onto Hybond$^+$ membranes (GE Amersham), hybridized with an end-labeled 375-nucleotide (nt) *sarA* mRNA probe, and washed as described previously (22). Protein bands binding to radiolabeled *sarA* mRNA were determined by tryptic digests followed by tandem mass spectrometry (MS/MS).

Preparation of cell lysates containing recombinant proteins in *E. coli*. For expression of putative RNA-binding proteins identified from mass spectrometry analysis (Table 2), genes encoding NWMN_0789, NWMN_1184, and NWMN_1985 from *S. aureus* strain Newman were cloned into pET15b or pET22b and induced with IPTG for overexpression using *E. coli* BL21(pLysS). For optimal expression, each clone was tested with different culture temperatures, including 37, 30, and 16°C and various final concentrations of IPTG at 0.1, 0.2, and 1 mM. Cells containing expressed proteins were harvested by centrifugation (20,200 × *g*, 5 min) after a 3-h induction period and treated with SDS-PAGE sample buffer.

Construction and purification of intact and truncated versions of CshA protein. The *cshA* open reading frame (ORF) was cloned to pET28a, using NdeI and BamHI enzymes and the following primer pair (5′-aaaC ATATGttgcaaaattttaaagaactagggatttcg-3′ and 5′-aaaGGATCCttatttttgatg

TABLE 2 Putative RNA-binding proteins identified by a tandem mass spectrometer[a]

Name/locus in Newman	Locus in N315	Mol mass (Da)	% detected by mass	Putative function(s)
Hypothetical protein NWMN_0192	*sa0248*	66,082	43.5	Glycosyl transferase group 2 family protein
Probable DEAD box ATP-dependent RNA helicase NWMN_1985	*sa1885*	56,941	36.0	ATP-dependent RNA unwinding splicing, ribosome biogenesis, and RNA degradation
Map-ND2C protein/NWMN_1872	*sa1751*	65,443	22.6	Binding ECM[b] and plasma
Aerobic glycerol-3-phosphate dehydrogenase/*glpD*/NWMN_1209	*sa1142*	64,361	23.0	DNA/RNA-binding repeats in PUR-α/β/γ and in hypothetical proteins
Protein map precursor (MHC class II analog protein) NWMN_1872	*sa1751*	65,443	10.7	Unknown function/S4 RNA-binding domain
UPF0051 protein NWMN_0789/*sufB*	*sa0778*	52,458	9.3	FeS assembly protein SufB
Hypothetical protein NWMN_1184	*sa1118* (*rnjB*)	62,473	4.8	RNA processing and degradation
ATP-dependent hsl protease ATP-binding subunit hslU NWMN_1164	*sa1097*	52,556	5.4	ATP-dependent protease ATP-binding subunit (*S. aureus* subsp. *aureus* TCH70)

[a] Sequence coverage and peptides are indicated. The gene name, locus, and proposed functions are as predicted in the NCBI and KEGG databases.
[b] ECM, extracellular matrix.

gtcagcaaatgtgcg-3′ [restriction sites are capitalized]). The recombinant plasmid from *E. coli* DH5α was transformed into *E. coli* Rosetta for protein expression. The *E. coli* construct was grown in LB containing 100 μg/ml kanamycin, and upon reaching an OD_{600} of ~0.7, induced with 0.2 mM IPTG for 3 h at 37°C. Cells were harvested by centrifugation (3,220 × *g*, 30 min), resuspended in a mixture of 20 mM Tris-HCl (pH 7.9), 500 mM NaCl, 20 mM imidazole, 1 mM dithiothreitol (DTT), 1 mM phenylmethylsulfonyl fluoride (PMSF), and 5% glycerol, and disrupted with a French press (10,000 lb/in^2, twice). After centrifugation (20,200 × *g*, 30 min), the insoluble fraction was resuspended in 5 ml of denaturing buffer containing 20 mM Tris-HCl (pH 7.9), 500 mM NaCl, 6 M guanine-HCl, and 2 mM DTT. To refold the protein, stepwise dialysis was performed, progressing from a high-denaturant condition (7 M urea, 20 mM Tris-HCl [pH 7.9], 500 mM NaCl, 20 mM imidazole, 3 h) to a nondenaturing condition (20 mM Tris-HCl [pH 7.9], 250 mM NaCl, overnight). To purify the protein, soluble protein fraction was applied to a nickel column, which was then washed, eluted with 500 mM imidazole following the manufacturer's instructions (Novagen), and dialyzed in a buffer containing 20 mM Tris-HCl (pH 7.9), 250 mM NaCl, and 5% glycerol. CshA protein purified in this manner was found to be functional with regard to helicase and ATPase activities (see Results below).

For the truncated proteins, an assortment of pET22b vectors containing PCR-generated truncated fragments of *cshA*, including the ATPase and the helicase domains and ending in a stop codon, were constructed (see Fig. 3A). (The primers for construction are available on request). The PCR products were digested with NdeI and BamHI and cloned to pET22b. All of the recombinant plasmids in *E. coli* DH5α were transformed into *E. coli* BL21(pLysS) for protein expression as described above.

RNA isolation and Northern blot analysis. Isolation of RNA and Northern blot hybridization were performed as previously described (23). In brief, overnight *S. aureus* cultures diluted 1:1,000 in TSB were grown at 37°C and induced with 1 mM IPTG to activate $MazF_{sa}$ expression at an OD_{650} of ~0.4. Cells were incubated for 30 min at 37°C and harvested at serial time points at 0, 1, 2, 5, and 10 min after rifampin treatment (200 μg/ml). Bacterial pellets were resuspended in 1 ml of TRIzol (Invitrogen) with 0.1-mm glass/zirconia beads, and RNA was extracted as described previously (23). Total RNA (10 or 25 μg) of each sample was applied to each lane of the RNA gel for Northern blotting as described previously (23).

Construction of *S. aureus* Newman Δ*cshA*::*kan* mutant and complemented mutant. Both the *cshA* mutant and the complemented mutant of ALC6094, a Newman derivative, were created as described previously (23).

Assays for ATPase and helicase activities. ATPase activity and the strand displacement assay for helicase activity were performed as described previously, with some modifications (28). Briefly, hydrolysis of radioactive [α-^{32}P]ATP to ADP was analyzed on thin-layer chromatography (TLC) plates. The reaction mixture contained increasing concentrations of CshA in the following buffer (10 μl): 20 mM Tris-HCl (pH 7.5), 50 mM potassium acetate, 5 mM magnesium acetate, 2 mM DTT, 0.1 mg/ml bovine serum albumin (BSA), and 10 μCi [α-^{32}P]ATP, with or without whole *S. aureus* total RNA. Reactions were stopped by adding a 10% volume of 0.5 M EDTA. For TLC, aliquots (5 μl) were spotted onto polyethylenimine-cellulose plates (EMD, Inc.) and separated in 0.15 M formic acid (pH 3.0) and 0.15 M LiCl.

For helicase activity assay, we deployed a 30-nt RNA (AAAAAUCGA AUCAUUAUUGAGTCGAGUAAA) and its partially complementary 29-nt-long DNA oligomer (GTAATAACTCAGCTCATTTCCTAGGAAA). The DNA oligonucleotide (3.3 μM) was then end labeled with 10 U of T4 polynucleotide kinase and 30 μCi of [γ-^{32}P]ATP for 30 min at 37°C (20-μl volume) and purified using an RNeasy MinElute cleanup kit (Qiagen). The duplex was formed by incubating 10 μM RNA with 10 μM unlabeled DNA oligonucleotide, 0.33 μM γ-^{32}P-labeled DNA oligonucleotide, 20 mM Tris base (pH 8.0), 200 mM potassium acetate, and 0.1 mM EDTA in a 25-μl volume, heated to 95°C for 30 s, gradually cooled to 45°C, and then slowly cooled to 4°C. For the reaction, the mixture containing 200 nM duplex, 5 μM unlabeled DNA oligonucleotide, 20 mM Tris base (pH 7.5), 50 mM potassium acetate, 5 mM magnesium acetate, 10 mM DTT, 0.1 mg/ml BSA, 10 U RNasin (Promega), various concentrations of CshA, and 1 mM ATP was incubated at 37°C for various times and then quenched at 4°C. Loading buffer (5 μl) containing 40% glycerol, 10 mM EDTA, 0.025% bromophenol blue, and 0.025% xylene cyanol blue was added, and the samples were resolved in 20% polyacrylamide gel (29:1), with the radioactive bands detected with a Storm 860 PhosphorImager (Molecular Dynamics) and quantified using the ImageQuant 5.2 software (Molecular Dynamics).

Cold-sensitive experiments. Parental *S. aureus* strain ALC6094, the Δ*cshA*::*kan* mutant, and the complemented mutant grown overnight at 37°C were diluted in fresh TSB to an OD_{650} of 0.05 and then grown at 25 or 37°C at 220 rpm. Triplicate samples were then taken serially for OD_{650} measurements to obtain the growth curve.

Bacterial growth and viability assay upon induction with $MazF_{sa}$. The parent ALC6094 strain, *cshA* mutant, and complemented mutant containing plasmid pG164::$mazF_{sa}$ were grown and induced with 1 mM IPTG for $MazF_{sa}$ expression. The control was cells with pG164 alone. The OD_{650} was then serially monitored for growth. In addition, cells were stained with the membrane-permeable vital stain Syto 9 and the membrane-impermeable dye propidium iodide following the instructions of the BacLight LIVE/DEAD kit (Invitrogen) (22). Briefly, Syto 9 dye and propidium iodide were mixed, diluted with filter-sterilized water, and added to a bacterial suspension at 100 μl/well. After incubation of the plate at room temperature in the dark for 15 min, the fluorescence intensities of live cells (excitation maximum/emission maximum [Ex/Em],

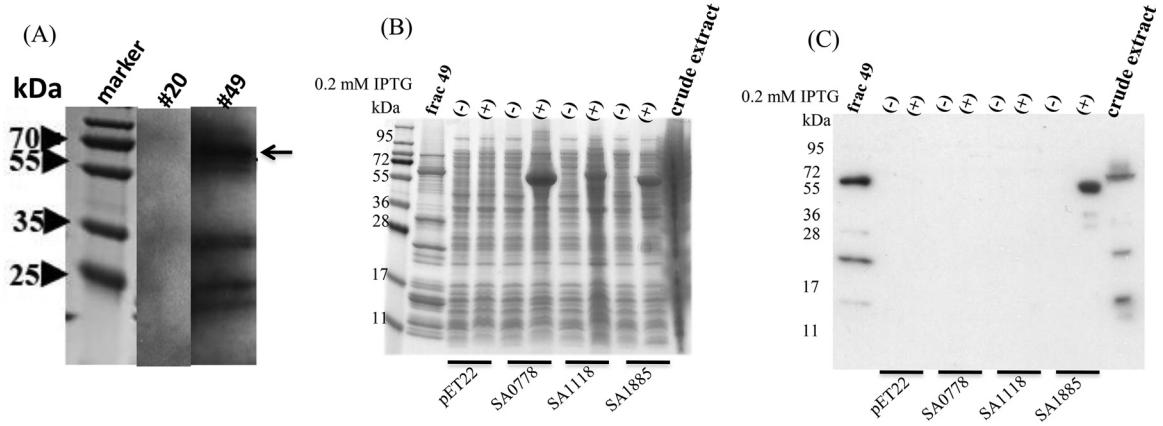

FIG 1 Binding of labeled *sarA* mRNA to *S. aureus* proteins. (A) Fractionated protein samples of *S. aureus* ALC6094 containing pG164-MazF$_{sa}$ with 1 mM IPTG from the heparin-Sepharose column were hybridized with [γ-^{32}P]ATP end-labeled *sarA* mRNA on Northwestern blots. A protein band of interest (~60 kDa) in fraction 49 is indicated by an arrow. (B) *E. coli* BL21 cell lysates expressing different ORFs from vectors pET22b(+), pET22b::*sa0778*, pET22b::*sa1118*, and pET22b::*sa1885* were analyzed on 16% SDS gel with (+) and without (−) induction with 0.2 mM IPTG. Two controls from MazF$_{sa}$-expressing *S. aureus* were used: crude extract collected after cell disruption and fraction 49, which represents one of the fractions from heparin-Sepharose column chromatography reactive with the *sarA* probe (A). (C) An identical gel transferred to a blot hybridized with the 375-nt *sarA* mRNA probe. *E. coli* BL21(*pLysS*) crude cell lysates harboring pET22b alone without IPTG did not react with the *sarA* mRNA probe (not shown).

485/530 nm) and dead cells (Ex/Em, 485/630 nm) were measured in a FL600 fluorescence reader (BioTek Instruments, Winooski, VT), using a standardized curve of the ratio of live to dead cells where fresh culture without MazF$_{sa}$ induction was defined as 100% live cells and culture heat killed at 60°C for 1 h was defined as dead cells (22).

NanoString nCounter assay and qRT-PCR. NanoString nCounter assays were performed as described previously (29). Our nCounter CodeSet consisted of oligonucleotides that assessed expression of 385 genes in a single experiment, the totality of sRNAs discovered in the genome of *S. aureus* N315 (30), all known virulence factors, regulator determinants, and genes involved in various stress responses, as well as housekeeping and reference genes allowing normalization. All oligonucleotides were designed by the NanoString algorithm to be complementary to their RNA target for 50 bases.

The strains tested in NanoString were wild-type ALC6094 and the Δ*cshA* strain containing the plasmid pG164::*mazF$_{sa}$*. Briefly, from an overnight culture, two 150-ml samples of fresh Muller-Hinton broth supplemented with 10 μg/ml chloramphenicol in 500-ml flasks were inoculated at an initial OD$_{650}$ of 0.0362. Cultures were grown at 37°C with agitation (250 rpm) until they had reached an OD$_{650}$ of 0.4, at which time, 1 mM IPTG was added to induce MazF$_{sa}$ expression. Suspensions were harvested at 0, 15, and 45 min upon MazF$_{sa}$ induction and subjected to total cellular RNA purification as described above. The mRNA counts were TMM (trimmed mean of M-values) normalized and then transformed into log$_2$ expression values with the voom function of the limma R package (31, 32). To detect differentially expressed transcripts, pairwise comparisons were performed and statistical significance ($P < 0.05$) determined, and the results were analyzed with the R limma package.

qRT-PCR analysis. Reverse transcription-quantitative PCR (qRT-PCR) was performed as previously described (33). Briefly, cDNA was obtained using qScript cDNA Supermix (Quanta Biosciences) and DNase I-treated RNA as a template. Following the manufacturer's instructions, PerfeCTa SYBR green FastMix (Quanta Biosciences) was used to generate standard curves of the cDNA concentration/crossing point (C_p) for the target genes and the reference genes, *gyrB* or 23S rRNA. Expression of the target genes was analyzed using the dilution for which the qRT-PCRs had the highest efficiency and reproducibility. The mean target transcriptional expression level for the three transcript measurements was calculated. The threshold cycle ($2^{-\Delta\Delta CT}$) method was used to calculate relative changes in gene expression, using triplicate samples. Roche's LightCycler 480 SW (version 1.5) software was used to analyze the qRT-PCRs. Control reaction mixtures containing master mix and primers but no cDNA were also analyzed.

RESULTS

Identification of putative protein(s) binding *sarA* mRNA. We previously proposed that RNA-binding proteins may be involved in conferring protection to selective mRNA against the endoribonucleolytic effect of the MazF$_{sa}$ toxin (22). To identify the protein, we fractionated crude extracts prepared from MazF$_{sa}$-inducing *S. aureus* ALC6096 cells using heparin-Sepharose column chromatography (27). These cellular extracts were electrophoretically resolved and hybridized with radiolabeled *sarA* mRNA (375 nt) in a Northwestern blot. The *sarA* mRNA probe hybridized with multiple protein bands, in a few cellular fractions that have been induced with IPTG for MazF$_{sa}$ expression in the region of ~60 kDa (Fig. 1A) compared with the noninduced control. A gel slice of a prominent band (indicated by an arrow in Fig. 1A) was cut, and the proteins were identified by mass spectrometry. Table 2 shows the proteins identified from the gel slice containing putative RNA binding and hypothetical proteins.

N-terminal His-tagged SA1885 (N315 genome) from *E. coli* BL21 binds to *sarA* mRNA. To confirm if the proteins identified (Table 2) bind to *sarA* mRNA, we expressed the hypothetical or putative RNA-binding proteins with IPTG induction (Fig. 1B) using pET22b or pET15b in *E. coli* BL21(pLysS) (see Materials and Methods). A Northwestern blot showed that only the *E. coli* crude extract that contained expressed NWMN_1985 (SA1885 with the N315 genome) was able to bind radiolabeled *sarA* mRNA, while others did not (Fig. 1C). We also examined the remaining proteins in Table 2 using this technique, and all failed to bind the *sarA* mRNA probe (data not shown). Homology search showed that *S. aureus* SA1885, with a predicted molecular mass of 56,941 Da (506 amino acids) and a pI of 9.49, is a putative DEAD box RNA helicase, an enzyme with distinct helicase and ATPase domains that unwinds double-stranded RNA in an ATP-dependent manner and possesses ATPase activity (34). Given its similarity (70%) and identity

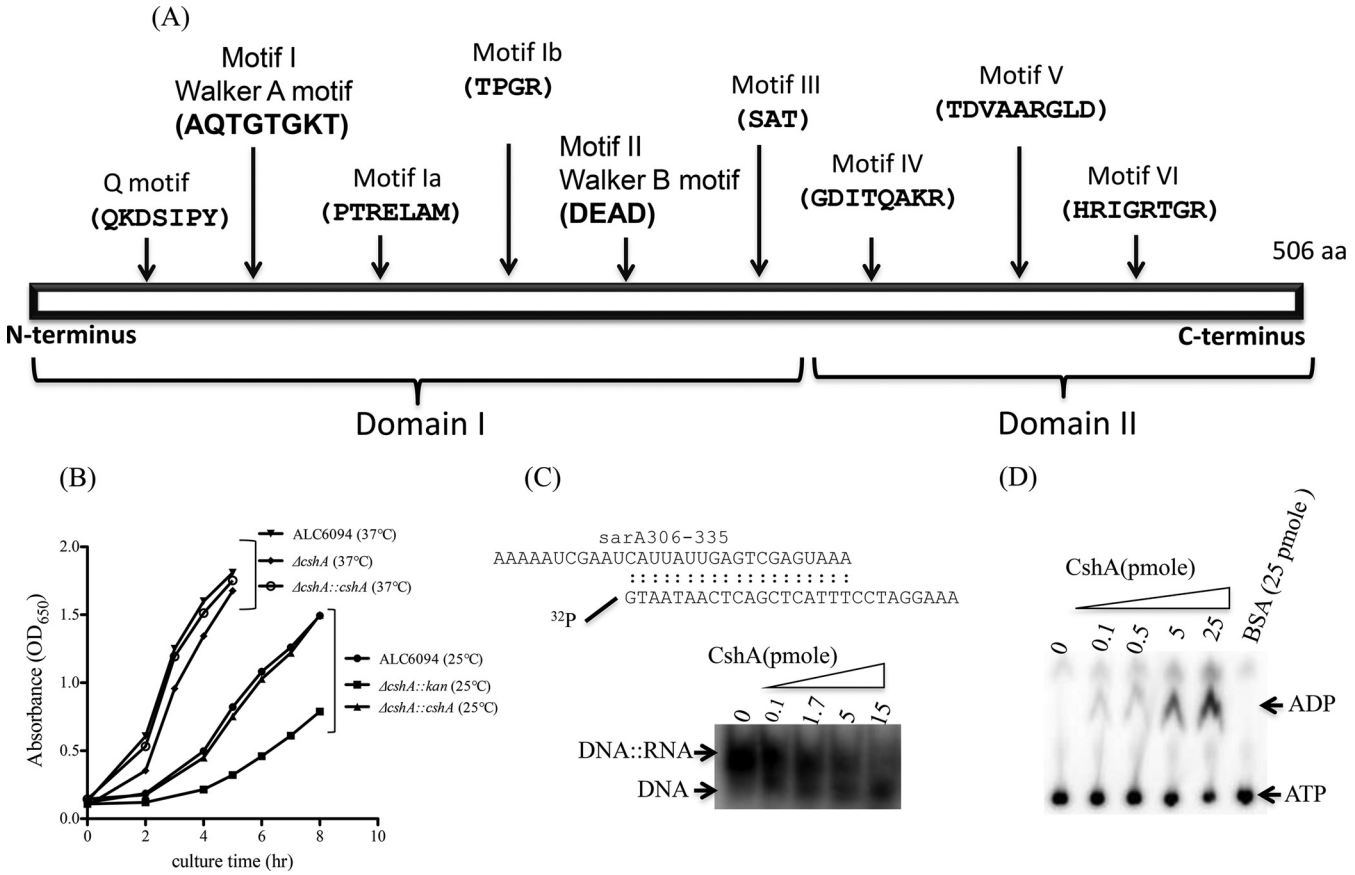

FIG 2 (A) Schematic depiction of domains and motifs of DEAD box RNA helicase CshA. Domains I and II, representing the ATPase and helicase domains, respectively, are bracketed at the bottom, and each motif is indicated by arrows on the top, with the relevant amino acid sequence of each motif presented. (B to D) Properties of RNA helicase CshA. (B) Growth of the parental, *cshA* mutant, and complemented mutant strains in TSB at 37 or 25°C, with OD_{650} measured serially. (C) The RNA helicase activity of CshA was measured using a DNA-RNA hybrid. The 29-base DNA oligomer was end labeled at the 5′ end and incubated with increasing concentrations of CshA. (D) ATPase activity of RNA helicase CshA was measured by conversion of ATP to ADP. [α-^{32}P]ATP was incubated with increasing concentrations of CshA (0.1 to 25 pmol), and BSA at 25 pmol was used as a control. The substrates were resolved on TLC plates as described in Materials and Methods.

(49%) to *B. subtilis* RNA helicase CshA (35), we have called this protein CshA, following the designation of Oun et al. (34).

CshA contains nine core motifs, Q, I, Ia, Ib, II, III, IV, V, and VI (Fig. 2A). The Walker A and B motifs, responsible for ATPase activity, are found in motifs I and II, respectively. Within the Walker B motif is the amino acid sequence D-E-A-D (Asp-Glu-Ala-Asp), thus conferring the denomination of "DEAD box" protein (36, 37). CshA has unique N- and C-terminal extensions that are not conserved, as has been found in other members of the DEAD box protein family (32). In particular, the C-terminal domain (~170 residues) has no homologous sequence as determined by BLASTP analysis (Fig. 2A).

CshA of *S. aureus* strain Newman has properties of an RNA helicase. To test whether *cshA*, encoding an RNA helicase, has an effect on cold sensitivity, we grew the *S. aureus* ALC6094 (parent), Δ*cshA*::*kan*, and complement mutant strains at 37 and 25°C. Growth of the mutant was greatly retarded in comparison to that of the parental and complemented strains at 25°C (Fig. 2B), while growth rates at 37°C were generally comparable among the three strains. These results indicated that CshA confers a cold sensitivity phenotype in *S. aureus*.

RNA helicases have been known to unwind double-stranded RNA (dsRNA) or RNA duplex as part of the secondary structures of RNA (38). To evaluate this, we randomly customized a 30-nt RNA, *sarA306*, spanning positions +306 to +335 from the *sarA* translational start site and a 29-nt DNA oligomer, 19 nt of which is complementary to the RNA template. The helicase activity of CshA was then assessed by its ability to displace labeled DNA strand from an RNA-DNA duplex (38, 39). The end-labeled DNA oligomer was designed to migrate faster on 20% native polyacrylamide gel than the labeled DNA-RNA duplex. As shown in Fig. 2C, CshA was able to displace the labeled DNA oligomer from the RNA-DNA duplex as the concentration of CshA was increased.

We also assessed the ATPase activity of purified CshA by determining the hydrolysis of labeled ATP to ADP. As seen in Fig. 2D, ADP was released from ATP on TLC plates with increasing concentrations of CshA in the presence of RNA (1 μg) (Fig. 2D, lanes 2 to ~5). In contrast, the control BSA protein (25 pmol) had no effect on the conversion of ATP to ADP (Fig. 2D, lane 6). Taken together, the above data confirmed CshA is a DEAD box RNA helicase.

C-terminal domain of CshA binds 375-nt *sarA* mRNA. To determine which domain of CshA is responsible for binding to

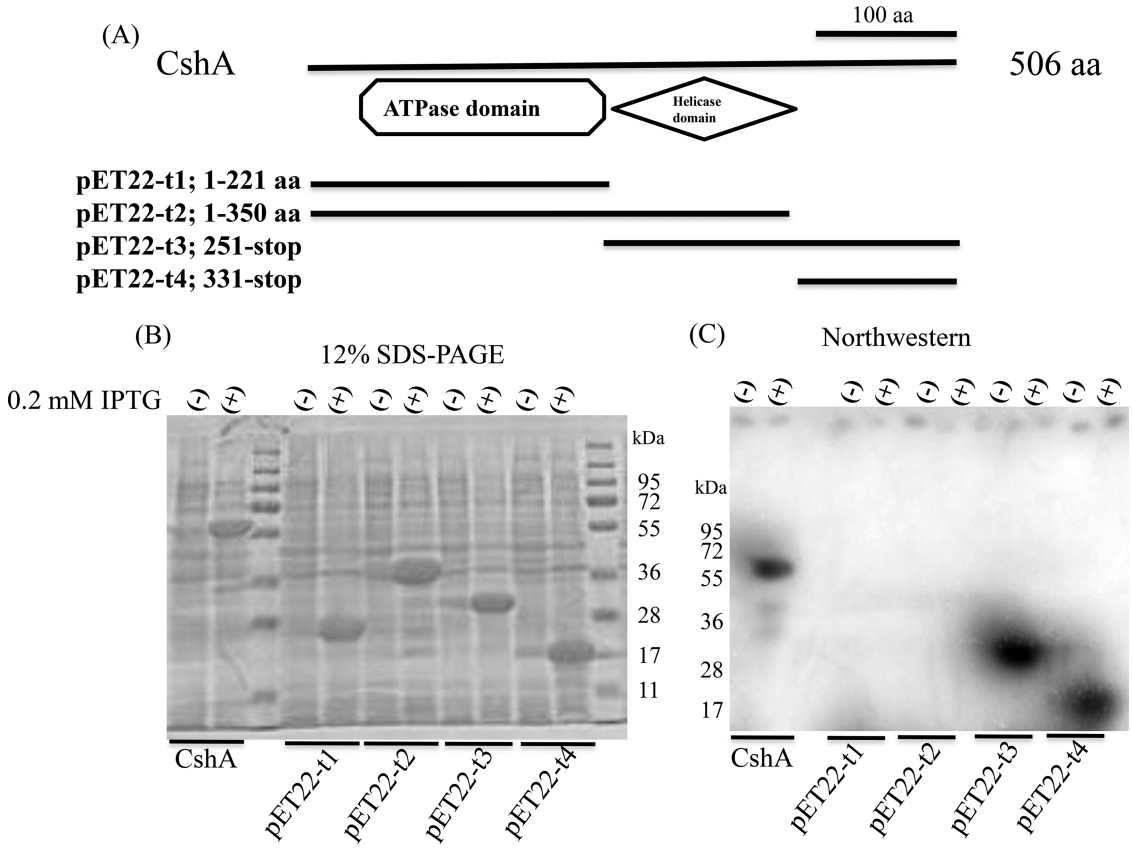

FIG 3 Interaction of *sarA* mRNA with truncated versions of CshA. (A) Depiction of the different truncated versions of CshA. Each truncated fragment was created by PCR, cloned to pET22b with NdeI and BamHI, and expressed using *E. coli* BL21(pLysS). (B) SDS-PAGE (12%) analyzing cell lysates before (at an OD_{600} of 0.7) and after addition of IPTG to a final concentration of 0.2 mM and grown for 3 h [indicated by (−) and (+), respectively]. (C) Northwestern blot showing labeled *sarA* mRNA hybridized to protein bands.

sarA mRNA, we prepared truncated versions of CshA expressed in *E. coli* as described in Materials and Methods (Fig. 3A). As seen in Fig. 3B, correct sizes of the truncated version of the protein were identified on SDS gels upon induction with IPTG. Cell lysates containing the truncated C-terminal domain of CshA were found to bind radiolabeled *sarA* mRNA on Northwestern blotting, while those expressing the N-terminal portion (ATPase domain) and the central portion (helicase domain) did not (Fig. 3C). These data indicated that only the C terminus of the RNA helicase CshA, representing the highly variable region of the molecule, is necessary for binding to *sarA* mRNA. As a control, we found the C terminus of NWMN_1461, another DEAD box RNA helicase, did not bind *sarA* mRNA (data not shown).

CshA protects *sarA* mRNA but not *spa* mRNA *in vivo*. Based on the binding of CshA to *sarA* mRNA on Northwestern blots (Fig. 1), we hypothesize that CshA may protect *sarA* mRNA (see the organization of the locus in Fig. 4A) from $MazF_{sa}$-mediated cleavage (22). To verify this, we analyzed two mRNA targets, *sarA* and *spa* mRNAs, with the former chosen for its protection from $MazF_{sa}$-mediated cleavage and the latter chosen for a lack of protection. With $MazF_{sa}$ induction, the *spa* transcript disappeared in the mutant and the parent and the complemented mutant (Fig. 4B), indicating that the *spa* transcript is not a selective target for protection by CshA against $MazF_{sa}$ cleavage *in vivo*.

The situation with *sarA* mRNA upon $MazF_{sa}$ induction is different. In contrast to *spa* (Fig. 4B), the *sarA* P3 and P1 transcripts were greatly enhanced in the parent and complemented mutant at 45 to 60 min after $MazF_{sa}$ induction compared to the absence of induction at time 0 min (Fig. 4C), similar to what has been described in our previous study (22). Importantly, the *sarA* P3 and P1 transcripts (Fig. 4A) were significantly reduced in the *cshA* mutant compared to the parent and the complemented mutant upon induction with IPTG (Fig. 4D and E). These data support the hypothesis that the RNA helicase CshA might confer specific protection for *sarA* mRNA, but not *spa* mRNA, against $MazF_{sa}$ cleavage *in vivo*.

Transcriptome of the *cshA* mutant using NanoString nCounter. Recognizing that CshA may protect "selective mRNA" from $MazF_{sa}$ cleavage, we examined transcripts that were decreased in the *cshA* mutant compared to the parental strain upon $MazF_{sa}$ induction with NanoString nCounter, a highly efficient and reliable method to measure transcripts of genes and sRNAs (29). Parental strain ALC6094, the *cshA* mutant, and the complemented mutant carrying the plasmid pG164::$mazF_{sa}$ were grown and induced with IPTG to express $MazF_{sa}$ at an OD_{650} of 0.4. At 15 and 45 min after $MazF_{sa}$ induction, cells were harvested and total cellular RNAs were extracted as described above. Seventeen out of 385 mRNA transcripts applied to the NanoString nCounter were decreased at 15 or 45 min in the *cshA* mutant upon MazF induction compared with the parental

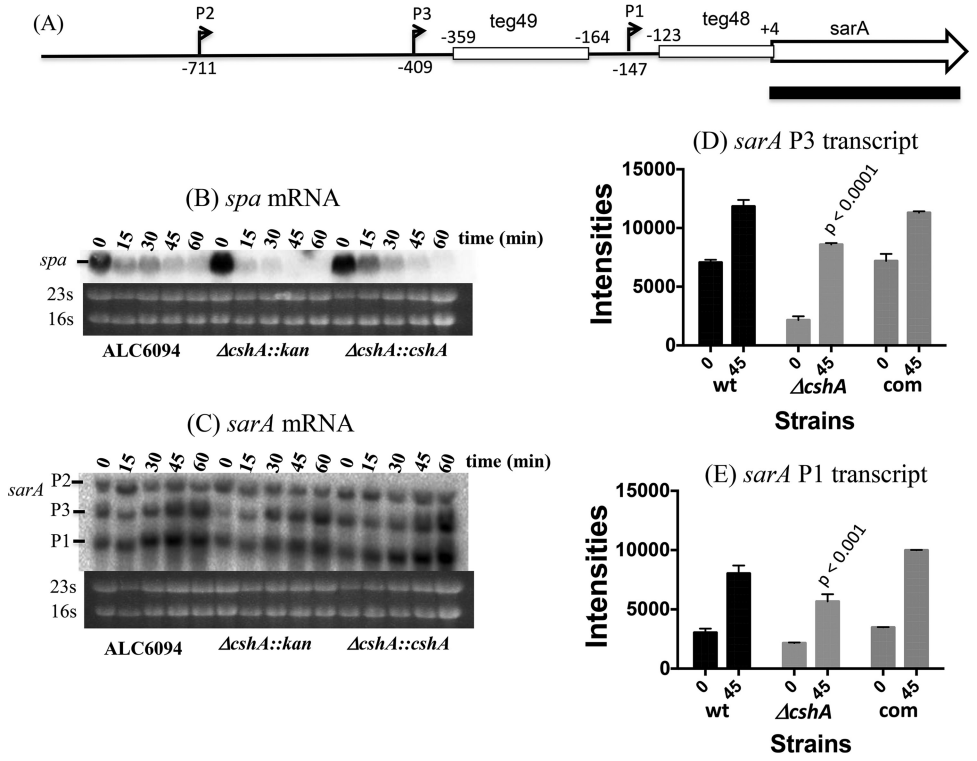

FIG 4 Northern blots of the parent ALC6094, *cshA* mutant, and complemented strains with the plasmid pG164::*mazF*$_{sa}$ probed with labeled *spa* and *sarA* mRNAs. (A) Map of the 5′-UTR, *sarA* transcripts, and *sarA* ORF. The transcript start sites of P2, P3, and P1 and two sRNAs, teg049 and teg048, are indicated as described previously (23). The *sarA* ORF (black bar) was used as a probe for Northwestern blotting assays. (B and C) Northern blots of parent, mutant, and complemented strains with plasmid pG164::*mazF*$_{sa}$ with IPTG induction probed with *spa* (B) or *sarA* (C) probe. (D and E) Quantification of *sarA* P3 (D) and P1 (E) transcripts in the parental strain and *cshA* mutant at 45 min upon MazF$_{sa}$ induction by ImageJ. The P3 and P1 transcripts prepared at an OD_{650} of 0.4 without MazF$_{sa}$ induction (at time 0) by IPTG were also included as controls. These experiments have been repeated at least three times, with one set of typical experiments shown. The *P* values of *sarA* P3 and P1 transcripts upon MazF$_{sa}$ induction were obtained by comparing the parent versus Δ*cshA* strain using analysis of variance (ANOVA) statistics.

strain (Table 3). Among these are genes involved in stress (*asp23*, *csbD*, and *cspA* to *-C*), secretion (*secY*), cell division (*ftsL*, *ftsW*, and *spoVG*), and gene regulation (*sarA*). The NanoString data on mRNA have been validated for many genes by qRT-PCR with normalization against *gyrB* or 23S RNA. As examples, *lctE* expression was not affected in the *cshA* mutant (Fig. 5A), whereas *secY* and *asp23* transcripts were significantly lower in the *cshA* mutant than in the parent (Fig. 5B and E). Very few metabolic and synthesis genes are decreased in the *cshA* mutant versus the parent. These data are consistent with the notion that CshA is likely involved in protection of specific transcripts that are required for cell survival under stress.

TABLE 3 Genes more abundant in the WT than in the *cshA* mutant upon MazF$_{sa}$ expression

Gene name	Fold change (WT vs *cshA* mutant)	Time (min)	*P*
asp23	6.4	15	0.002
clfA	4.7	15	0.004
csbD	4.4	15	0.006
cspA	1.9	15	0.049
cspB	2.8	45	0.011
cspC	1.8	45	0.049
dltB	2.1	45	0.014
dltC	2.2	45	0.013
dltD	2.0	45	0.024
ebpS	2.2	15	0.047
folD	1.9	15	0.048
ftsL	2.7	15	0.013
ftsW	2.0	45	0.038
sarA	2.9	15	0.010
secY	1.6	15	0.050
spoVG	2.9	15	0.010
treP	2.2	45	0.050

Besides mRNA, we also examined the transcription of 85 sRNAs in the *S. aureus* genomes (based on our *PloS One* article, some of the teg sRNAs presenting size <100 nt or teg showing high homology but failed to be assessed by RNA-Seq) (30). Among these, 22 sRNAs were expressed at a lower level in the *cshA* mutant versus the parent under MazF$_{sa}$ induction (Table 4), thus implying protection of a large number of sRNAs by CshA. Of interest are teg049 and teg048, both of which are found within the 5′ untranscribed region (UTR) of *sarA* (Fig. 4A) (23). The *sarA* P1 and P3 transcripts were also protected by CshA upon MazF$_{sa}$ induction, concordant with the Northern blot data (Fig. 4C). Notably, teg017, an sRNA adjacent to *cshA* in the genome, was also protected (Table 4). The NanoString data on sRNA were subsequently confirmed by qRT-PCR with normalization against *gyrB* or 23S RNA. More specifically, the teg049 and teg057 transcripts (Fig. 5D and E) were expressed at a reduced level in the *cshA* mutant versus the parent, while expression of teg058, a nonpro-

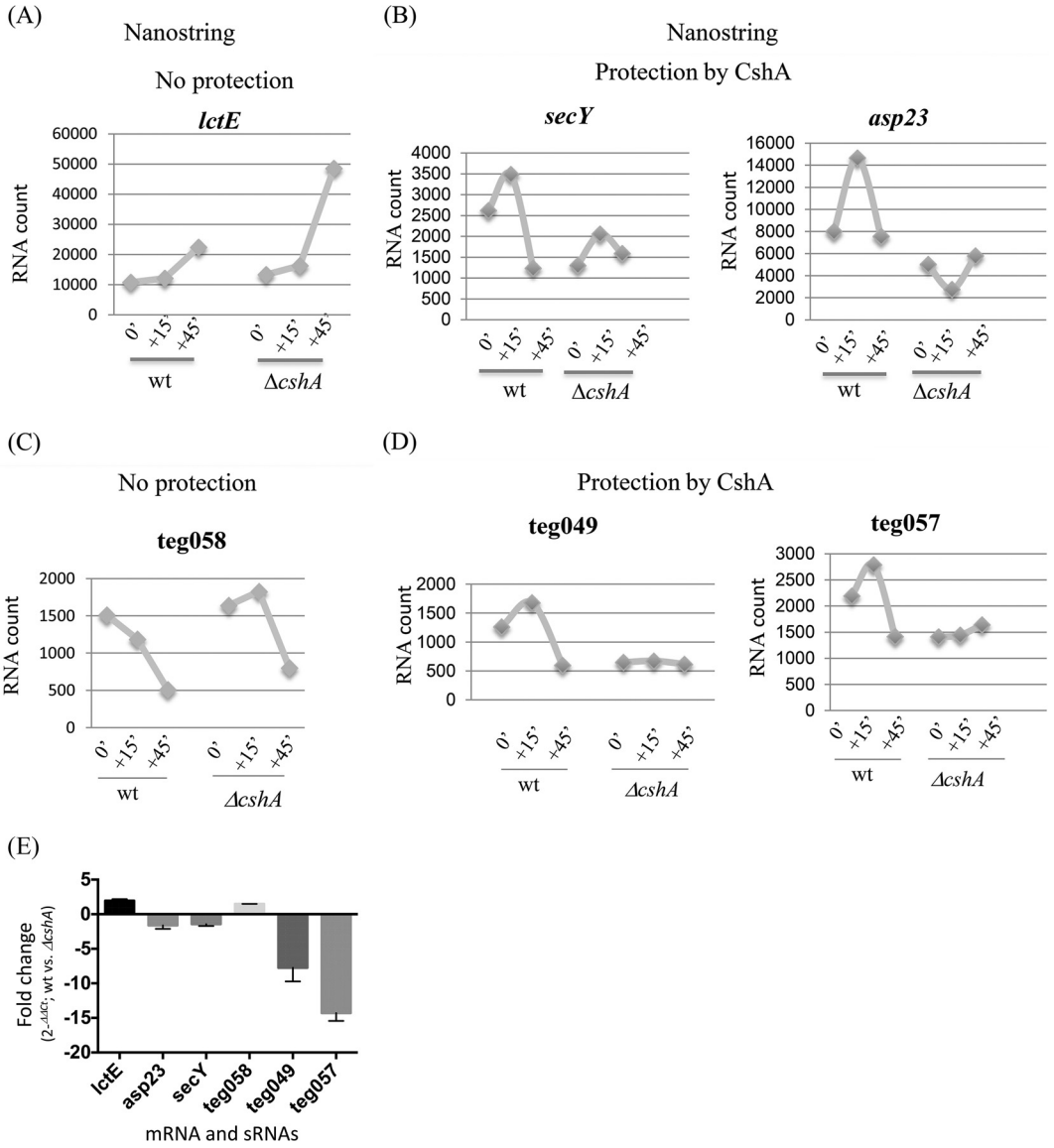

FIG 5 Analysis of the transcriptome by NanoString nCounter and selective confirmation by qRT-PCR. Expression of mRNAs (A and B) and sRNAs (C and D) was measured by NanoString nCounter and confirmed by qRT-PCR (E). For qRT-PCR, each RNA sample was collected at 15 min after 1 mM $MazF_{sa}$ induction and processed following the manufacturer's instructions. Each $\Delta\Delta C_T$ value was calculated as the ΔC_T of the parent minus the ΔC_T of the *cshA* mutant upon $MazF_{sa}$ induction. The fold change was then calculated as $2^{-\Delta\Delta CT}$. Obtained positive and negative values are indicative of increased and decreased expression of transcripts, respectively (E). Two mRNAs, *secY* and *asp23*, and two sRNAs, teg049 and teg057, that were decreased in expression in the *cshA* mutant compared to the parent were chosen for the qRT-PCR data. We also used *lctE* and teg058 as the mRNA and sRNA controls, respectively. For qRT-PCR, RNA samples were prepared from cells that were harvested 15 min after addition of 1 mM IPTG to cultures at an OD_{650} of 0.4. The data were normalized against 23 sRNA or *gyrB* as reference transcripts for the qRT-PCR.

tected sRNA, was modestly increased in the *cshA* mutant (Fig. 5C and E).

teg049 expression after rifampin treatment. Small RNA teg049, located within the *sarA* P3-P1 promoter region, is 196 nt long and is transcribed in the same direction as the *sarA* P3 transcript (Fig. 4A) (23). We have previously shown that *cshA* is required for the generation of sRNA teg049 in *S. aureus*, presumably via site-specific cleavage of the *sarA* P3 transcript by host endoribonuclease (23). Given that Hfq of *S. aureus*, unlike its Gram-negative counterpart, did not display a major physiologic role (40), we wanted to determine if CshA contributes to the stability of sRNA teg049 by measuring its half-life in the presence of rifampin, which halts *de novo* synthesis of the transcript. The decay of the mRNAs was monitored by Northern blotting of total cellular RNA isolated from different time points (1, 3, 5, 10, and 15 min) after the addition of rifampin, as previously described (21). As shown in Fig. 6, the half-life of teg049 was significantly reduced in the *cshA* mutant compared with the parental and the complemented strains, with expression of teg049 significantly reduced at 1 min after rifampin treatment, while the transcript was prominently displayed in the parent and complemented mutant at the same time point.

TABLE 4 sRNAs more abundant in the WT than in the *cshA* mutant under $MazF_{sa}$ induction

sRNA	Location (NC_002745)	Flanking gene(s)	Length (nt)	Fold change for WT vs *cshA* (time in min)[a]
teg006	1399488–1399659	*sa1224*, *lysC*	171	3.2 (15)
teg008	1856495–1856645	Truncated *sa*, *tnp*	150	2.0 (15)
teg017	2135748–2135855	*tnp*, *sa1885*	107	2.0 (15)
teg021	2225691–2225573	*glmM*, *fmtB*	118	2.3 (15)
teg023	2353800–2353590	*sa2094*, *saS083*	210	2.5 (15)
teg027	2437048–2435872	*sa2169*, *sa2168*	1,176	3.2 (45)
teg040	407923–407503	*sa0348*, *sa0347*	420	3.0 (15)
teg041	470637–470841	*saS014*, *ndhF*	204	2.6 (45)
teg042	501430–501682	*sa0434*, *sa0435*	252	2.0 (45)
teg044	540718–540943	*sa0468*, *ftsH*	225	1.8 (45)
teg048	666844–666718	*sa0574*, *sarA*	126	2.7 (15)
teg049	667114–666952	*sa0574*, *sarA*	162	2.7 (15)
teg052	875399–875515	*saS023*, *sa0769*	116	2.5 (15)
teg054	1012987–1012840	*sa0892*, *sa0891*	147	4.0 (15)
teg057	1127112–1127350	*uvrC*, *sdhC*	238	2.2 (15)
teg061	1245093–1245202	*codY*, *rpsB*	109	2.3 (15)
teg075	1828607–1828451	*sa1590*, *ribD*	118	2.2 (45)
teg076	430826–431048	*sa0372*, *xprT*	222	2.2 (15)
teg088 (*rsaA*)	637124–637268	*sa0543*, *sa0544*	144	2.3 (15)
teg091 (*rsaD*)	696007–695896	*sa0601*, *sa0600*	111	3.7 (15)
teg36as[b]	2353116–2352665	*ssaA*	448	2.0 (15)
teg40as[b]	859910–859611	*sa0751*	299	3.2 (15)

[a] *P* values for the fold changes in these sRNAs are less than 0.05.
[b] teg36as and teg40as are antisense sRNAs. The locations of each of these sRNAs are indicated by a single flanking gene.

ImageJ analysis followed by deduction of half-lives allowed us to estimate the half-lives of teg049 to be ~1 min and ~3 min in the *cshA* mutant and the parental strain, respectively. This result is consistent with the notion that CshA likely stabilizes the sRNA teg049, which in turn confers protection for the *sarA* P3 transcript against $MazF_{sa}$ cleavage, as has been described previously (23).

Mutation of *cshA* affects growth and cell viability. Overexpression of $MazF_{sa}$ has been shown by us to induce cell stasis and growth arrest rather than cell death (21). If our hypothesis that CshA serves to protect some of the mRNAs from cleavage by activated $MazF_{sa}$ (e.g., *sarA* mRNA) is correct, one would predict that activation of $MazF_{sa}$ in a *cshA* mutant would render the mutant cells less viable than the parental cells, where there is selective mRNA protection to maintain viability. In the absence of ectopic $MazF_{sa}$ induction, the CFU counts of the *cshA* mutant were comparable to those of the parent and the complemented mutant, consistent with what we have reported previously (21; data not shown). Upon $MazF_{sa}$ induction, all three strains exhibited reductions in CFU counts, but the reduction was more dramatic in the *cshA* mutant than with the parent and complemented mutant (Fig. 7A). More specifically, the *cshA* mutant displayed at least a 6-log reduction in CFU counts at 45 min versus a 2-log reduction in the parent and complemented mutant after $MazF_{sa}$ induction. This was confirmed by plate counting of the *cshA* mutant versus the parent (Fig. 7B).

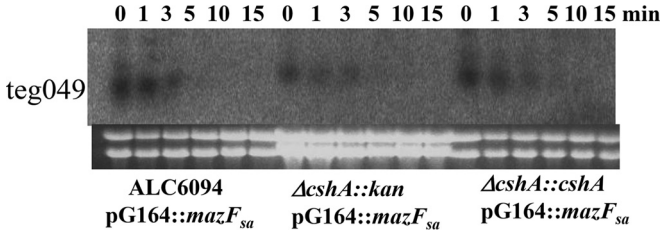

FIG 6 Decay of sRNA teg049 upon blocking *de novo* RNA synthesis with rifampin. *S. aureus* ALC6094, the *cshA* mutant, and the complemented mutant harboring pG164-*mazFsa* (His_6) were incubated with 1 mM IPTG upon reaching an OD_{650} of 0.4. Cells were then harvested at serial time points at 0, 1, 3, 5, 10, and 15 min after addition of rifampin (200 μg/ml). RNA was extracted and subjected to Northern blots with radiolabeled teg049 probe. The loading of RNA from the *cshA* mutant was higher than that in the parent to increase teg049 signal, while 23S and 16S rRNAs served as the internal loading controls.

To determine whether the *cshA* mutant cells are simply nonreplicative or dead, the induced and uninduced cultures were further examined for viability with a BacLight LIVE/DEAD bacterial viability assay kit (Molecular Probes). In agreement with prior results (21), both the parental and complemented mutant cells showed almost 100% viability, as detected by Syto 9 stain, even at 60 min postinduction (Fig. 7C). In fact, both of these strains grew slightly upon examination at 120 min. In contrast, the viability of the *cshA* mutant dropped significantly to ~40% of the preinduction level, even at 15 min postinduction, and was maintained there for an extended postinduction period (Fig. 7C). These results suggest that CshA plays a critical role in survival of *S. aureus* cells that are undergoing stasis upon $MazF_{sa}$ induction.

DISCUSSION

In previous studies, we have shown that *S. aureus* likely undergoes bacteriostasis by protecting selective mRNAs, including those of housekeeping genes and a global regulator (i.e., *sarA* mRNA), with RNA-binding proteins upon induction of $MazF_{sa}$ expression *in vivo* (22). In this study, we have used *sarA* mRNA as a probe in Northwestern blots to identify CshA, a DEAD box RNA helicase, which plays an *in vivo* role in protecting a modest number of mRNAs and a relatively large number of sRNAs from $MazF_{sa}$-mediated endoribonucleolytic cleavage.

Several lines of evidence suggest that CshA is a DEAD box RNA

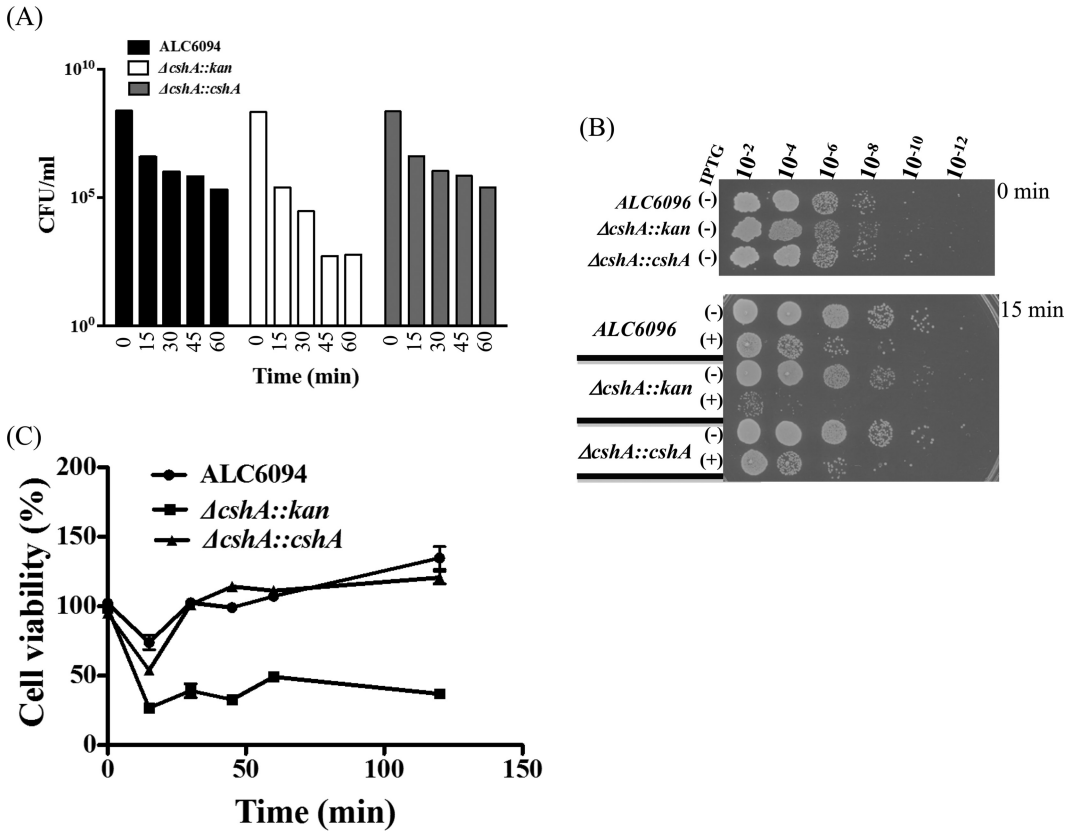

FIG 7 CFU counts and viability of the *cshA* mutant after ectopic $MazF_{sa}$ expression. (A) CFU counts of the parent ALC6094, *cshA* mutant, and complemented mutant harboring pG164-*mazF*$_{sa}$ (His_6) with 1 mM IPTG induction at an OD_{650} of 0.4. Cells were taken at various time points, and CFU were counted by plating on TSA. (B) Cell dilutions were plated at 0 and 15 min following 1 mM IPTG induction. (C) Relative cell viability of the parent, mutant, and complemented mutant containing pG164-*mazF*$_{sa}$. Cultures induced at an OD_{650} of ~0.4 with and without 1 mM IPTG were assessed for cell viability with a LIVE/DEAD BacLight bacterial viability kit at the indicated time points, as described in Materials and Methods. The percentage of viable cells from the induced culture at each time point was compared to that of an uninduced culture to arrive at the relative cell viability. The results represent the average from three similar independent experiments. Error bars show standard deviations.

helicase (41). First, CshA comprises nine conserved amino acid motifs commonly found in many RNA helicases (Fig. 2A). Second, the *cshA* mutant exhibits cold sensitivity to growth at 25°C (Fig. 2B) (42). Third, it binds to RNA duplex (data not shown), possesses helicase activity by displacing labeled DNA from an RNA-DNA duplex, and engenders ATPase activity (Fig. 2C and D) (40, 41). Additional studies revealed that CshA requires RNA duplex structure that is at least over 15 nt in length for interaction (data not shown).

Analysis of the C terminus of CshA reveals divergence from other RNA helicases. More specifically, BLAST search with the C-terminal region of CshA corresponding to residues 331 to 506 fails to unearth any significant homology to other protein coding regions. Interestingly, *E. coli* cell lysates expressing two truncated versions of CshA containing the unique C terminus, but not the N terminus or the central domain of the protein, hybridized to the labeled *sarA* mRNA (Fig. 3A and C). A recent study showed that the C terminus of *cshA* in *S. aureus* played critical roles in bulk RNA turnover and interaction with the degradosome (43). This finding is of interest since the highly variable C terminus may also confer RNA binding specificity and help explain why CshA only protects some of the mRNAs and sRNA *in vivo* upon activation of $MazF_{sa}$ in *S. aureus*.

As an RNA helicase, CshA is normally part of the RNA degradosome in Gram-positive bacteria from *Bacillus subtilis* (44) and *S. aureus* (45). Inactivation of *cshA* is predicted to augment transcript levels of genes that are destined for degradation, as has been seen with the *spa* transcript at time 0 (Fig. 4B). Based on our NanoString analysis with the *cshA* mutant (Fig. 5 and 6 and Tables 3 and 4), it would appear that CshA may offer protection to a number of specific mRNA and a relatively large number sRNAs under $MazF_{sa}$ induction. Of interest are the *sarA* P3 and P1 mRNAs as well as teg049 and teg048, two sRNAs between the P3 and P1 promoters and between P1 and the *sarA* translation start site, respectively, which were diminished in the *cshA* mutant compared with those of the parental strain under $MazF_{sa}$ induction (Fig. 4 and 5 and Tables 3 and 4) (23). IPTG induction of $MazF_{sa}$ enhanced the expression of *sarA* P3 and P1 transcripts (Fig. 4C at 0 versus 30, 45, and 60 min) and teg049 (data not shown) in the parental strain, while these transcripts were decreased at 45 and 60 min postinduction in the *cshA* mutant on Northern blots (Fig. 4C) (23). The above trend was also verified with NanoString nCounter and qRT-PCR analyses (Tables 3 and 4 and Fig. 5). These results are consistent with the notion that the DEAD box RNA helicase CshA confers protection to selective mRNAs and a large number

of sRNAs, likely to maintain viability of $MazF_{sa}$-induced *S. aureus* cells during periods of stress (21, 22).

A common mechanism by which stability is bestowed upon sRNA is due to an RNA chaperone protein such as Hfq (46). However, it has been shown in *S. aureus* that an *hfq* mutation did not result in any major phenotypic alterations (40). We thus suspect sRNAs such as teg049 may be protected by CshA. One mechanism of protection is the prolongation of half-life conferred by the RNA-binding protein. Northern blot studies confirmed that the half-life of teg049 was indeed reduced in the *cshA* mutant compared with those in the parent and complemented mutant, thus confirming that CshA likely imparts stability to sRNAs such as teg049.

teg049, residing between the *sarA* P3 and P1 promoters, is predicted to contain two stem-loop structures, HP1 and HP2, the former appearing to be critical for the proper processing of the *sarA* P3 transcript by host RNase to generate teg049 (23). In *E. coli*, RNase III is an endoribonuclease that cleaves double-stranded RNA and purportedly plays a broad role in mRNA processing, turnover and stability of many mRNAs and sRNAs (46, 47). In *S. aureus*, RNase III has been shown to be involved in regulating the turnover of mRNAs and noncoding RNAs (48, 49). RNase III also likely targets the 5′-overlapping regions of divergent mRNAs to generate species with shorter or even leaderless 5′ UTRs (50). In this regard, we have indirect evidence to suggest that CshA may bind *sarA* P3 mRNA to enable specific processing by RNase III to yield teg049.

We have also shown here that CshA plays a critical role in cell viability and survival in the context of $MazF_{sa}$ overexpression (Fig. 7). Remarkably, the *cshA* mutant yielded far fewer CFU counts than those of the parent and the complemented mutant even at 15 min after $MazF_{sa}$ induction (Fig. 7B). This discrepancy in CFU counts between the mutant and the parent (also the complemented mutant) extends to over a 4-log difference in CFU counts at 1 h postinduction (Fig. 7A). More specifically, there was only $\sim 5 \times 10^2$ CFU/ml of the mutant at 1 h postinduction, while those of the corresponding parent and complemented mutant approached $\sim 10^6$ CFU/ml. In contrast to the wild type, which was still viable after $MazF_{sa}$ induction (Fig. 7C), only ~40% of the *cshA* mutant cells remained viable, as confirmed by the BacLight LIVE/DEAD kit. These data thus indicated that CshA plays a pivotal role in *S. aureus* survival upon exposure to $MazF_{sa}$ during stress (10, 17). The physiologic basis of this mode of survival is likely attributable to the protective role of CshA on some essential mRNA and a large number of sRNAs, as we have demonstrated above.

Although CshA likely protects *sarA* P3 and P1 transcripts *in vivo*, we were not able to demonstrate that CshA can protect the *sarA* transcript from the endoribonucleolytic effect of $MazF_{sa}$ *in vitro* (data not shown). This could be explained by the possibility that CshA is a necessary but not sufficient condition for protection of *sarA* mRNA *in vivo*, and it is likely that additional proteins may be required for this protective effect in *S. aureus* cells. This conjecture was supported by our Northwestern blot data where there are additional bands of hybridization to the *sarA* probe besides CshA (Fig. 1A). It is plausible that these proteins may form a macromolecular complex to protect specific mRNAs or sRNAs from degradation. We have also ruled out the role of Hfq in this protective complex because Hfq did not bind *sarA* mRNA and a mutation in *hfq* did not appear to contribute to selective mRNA protection upon $MazF_{sa}$ induction (data not shown). Alternatively, the *sarA* mRNA may adopt a different secondary configuration *in vivo* (e.g., duplex formation promoted by other proteins, including CshA) to resist the endoribonucleolytic effect of $MazF_{sa}$.

Besides CshA, there is an additional DEAD box RNA helicase, SA1387 (NWMN_1461), in *S. aureus*. This protein was also identified as a *sarA* mRNA-binding protein on Northwestern blots (data not shown). Like CshA, CshB, at ~50 kDa, has inherent RNA-binding and ATPase activities but no obvious helicase activity (data not shown). Unlike CshA, the C terminus of CshB does not bind *sarA* mRNA (data not shown), thus suggesting that CshB is likely functionally distinct from CshA. Whether CshB partners with CshA to protect selective mRNAs or sRNAs warrants further investigation.

ACKNOWLEDGMENTS

This work was supported by grants AI106937 from the National Institutes of Health (to A.C.) and 31003A_153474/1 from the Swiss National Science Foundation (to P.F.).

FUNDING INFORMATION

HHS | NIH | National Institute of Allergy and Infectious Diseases (NIAID) provided funding to Ambrose Cheung under grant number AI91801. HHS | NIH | National Institute of Allergy and Infectious Diseases (NIAID) provided funding to Ambrose Cheung under grant number AI106937.

REFERENCES

1. **Ogura T, Hiraga S.** 1983. Partition mechanism of F plasmid: two plasmid gene-encoded products and a cis-acting region are involved in partition. Cell **32:**2351–2360.
2. **Yarmolinsky MB.** 1995. Programmed cell death in bacterial populations. Science **267:**836–837. http://dx.doi.org/10.1126/science.7846528.
3. **Donegan NP, Cheung AL.** 2009. Regulation of the *mazEF* toxin-antitoxin module in *Staphylococcus aureus* and its impact on *sigB* expression. J Bacteriol **191:**2795–2805. http://dx.doi.org/10.1128/JB.01713-08.
4. **Engelberg-Kulka H, Sat B, Reches M, Amitai S, Hazan R.** 2004. Bacterial programmed cell death systems as targets for antibiotics. Trends Microbiol **12:**66–71. http://dx.doi.org/10.1016/j.tim.2003.12.008.
5. **Gerdes K, Christensen SK, Lobner-Olesen A.** 2005. Prokaryotic toxin-antitoxin stress response loci. Nat Rev Microbiol **3:**371–382. http://dx.doi.org/10.1038/nrmicro1147.
6. **Grønlund H, Gerdes K.** 1999. Toxin-antitoxin systems homologous with *relBE* of *Escherichia coli* plasmid P307 are ubiquitous in prokaryotes. J Mol Biol **285:**1401–1415. http://dx.doi.org/10.1006/jmbi.1998.2416.
7. **Mittenhuber G.** 1999. Occurrence of MazEF-like antitoxin/toxin systems in bacteria. J Mol Microbiol Biotechnol **1:**295–302.
8. **Pandey DP, Gerdes K.** 2005. Toxin-antitoxin loci are highly abundant in free-living but lost from host-associated prokaryotes. Nucleic Acids Res **33:**966–976. http://dx.doi.org/10.1093/nar/gki201.
9. **Van Melderen L.** 2010. Toxin-antitoxin systems: why so many, what for? Curr Opin Microbiol **13:**781–785. http://dx.doi.org/10.1016/j.mib.2010.10.006.
10. **Engelberg-Kulka H, Amitai S, Kolodkin-Gal I, Hazan R.** 2006. Bacterial programmed cell death and multicellular behavior in bacteria. PLoS Genet **2:**e135. http://dx.doi.org/10.1371/journal.pgen.0020135.
11. **Hazan R, Sat B, Engelberg-Kulka H.** 2004. *Escherichia coli mazEF*-mediated cell death is triggered by various stressful conditions. J Bacteriol **186:**3663–3669. http://dx.doi.org/10.1128/JB.186.11.3663-3669.2004.
12. **Hazan R, Engelberg-Kulka H.** 2004. *Escherichia coli mazEF*-mediated cell death as a defense mechanism that inhibits the spread of phage P1. Mol Genet Genomics **272:**227–234.
13. **Hayes CS, Sauer RT.** 2003. Toxin-antitoxin pairs in bacteria: killers or stress regulators? Cell **112:**2–4. http://dx.doi.org/10.1016/S0092-8674(02)01282-5.
14. **Sat B, Hazan R, Fisher T, Khaner H, Glaser G, Engelberg-Kulka H.** 2001. Programmed cell death in *Escherichia coli*: some antibiotics can trigger *mazEF* lethality. J Bacteriol **183:**2041–2045. http://dx.doi.org/10.1128/JB.183.6.2041-2045.2001.
15. **Sat B, Reches M, Engelberg-Kulka H.** 2003. The *Escherichia coli mazEF*

suicide module mediates thymineless death. J Bacteriol **185:**1803–1807. http://dx.doi.org/10.1128/JB.185.6.1803-1807.2003.
16. **Aizenman E, Engelberg-Kulka H, Glaser G.** 1996. An *Escherichia coli* chromosomal "addiction module" regulated by guanosine 39,59-bispyrophosphate: a model for programmed bacterial cell death. Proc Natl Acad Sci U S A **93:**6059–6063. http://dx.doi.org/10.1073/pnas.93.12.6059.
17. **Donegan NP, Thompson ET, Fu Z, Cheung AL.** 2010. Proteolytic regulation of toxin-antitoxin systems by ClpPC in *Staphylococcus aureus*. J Bacteriol **192:**1416–1422. http://dx.doi.org/10.1128/JB.00233-09.
18. **De la Cruz MA, Zhao W, Farenc C, Gimenez G, Raoult D, Cambillau C, Gorvel JP, Méresse S.** 2013. A toxin-antitoxin module of Salmonella promotes virulence in mice. PLoS Pathog **9:**e1003827. http://dx.doi.org/10.1371/journal.ppat.1003827.
19. **Ramage HR, Connolly LE, Cox JS.** 2009. Comprehensive functional analysis of Mycobacterium tuberculosis toxin-antitoxin systems: implications for pathogenesis, stress responses, and evolution. PLoS Genet **5:**e1000767. http://dx.doi.org/10.1371/journal.pgen.1000767.
20. **Zhang Y, Zhang J, Hoeflich KP, Ikura M, Qing G, Inouye M.** 2003. MazF cleaves cellular mRNAs specifically at ACA to block protein synthesis in *Escherichia coli*. Mol Cell **12:**913–923. http://dx.doi.org/10.1016/S1097-2765(03)00402-7.
21. **Fu Z, Donegan NP, Memmi G, Cheung AL.** 2007. Characterization of $MazF_{sa}$, an endoribonuclease from *Staphylococcus aureus*. J Bacteriol **189:**8871–8879. http://dx.doi.org/10.1128/JB.01272-07.
22. **Fu Z, Tamber S, Memmi G, Donegan NP, Cheung AL.** 2009. Overexpression of $MazF_{sa}$ in *Staphylococcus aureus* induces bacteriostasis by selectively targeting mRNAs for cleavage. J Bacteriol **191:**2051–2059. http://dx.doi.org/10.1128/JB.00907-08.
23. **Kim S, Reyes D, Beaume M, Francois P, Cheung A.** 2014. Contribution of teg049 small RNA in the 5′ upstream transcriptional region of *sarA* to virulence in *Staphylococcus aureus*. Infect Immun **82:**4369–4379. http://dx.doi.org/10.1128/IAI.02002-14.
24. **Novick RP.** 1990. Molecular biology of the staphylococci, p 1–40. VCH Publishers, New York, NY.
25. **Baba T, Bae T, Schneewind O, Takeuchi F, Hiramatsu K.** 2008. Genome sequence of *Staphylococcus aureus* strain Newman and comparative analysis of staphylococcal genomes: polymorphism and evolution of two major pathogenicity islands. J Bacteriol **190:**300–310. http://dx.doi.org/10.1128/JB.01000-07.
26. **Sambrook J, Fritsch EF, Maniatis T.** 1989. Molecular cloning: a laboratory manual, 2nd ed. Cold Spring Harbor Laboratory Press, New York, NY.
27. **Kim S, Wolyniak MJ, Staab JF, Sundstrom P.** 2007. A 368-base-pair *cis*-acting *HWP1* promoter region, HCR, of *Candida albicans* confers hypha-specific gene regulation and binds architectural transcription factors Nhp6 and Gcf1p. Eukaryot Cell **6:**693–709. http://dx.doi.org/10.1128/EC.00341-06.
28. **Cordin O, Tanner NK, Doère M, Linder P, Banroques J.** 2004. The newly discovered Q motif of DEAD-box RNA helicases regulates RNA-binding and helicase activity. EMBO J **23:**2478–2487. http://dx.doi.org/10.1038/sj.emboj.7600272.
29. **Beaume M, Hernandez D, Docquier M, Delucinge-Vivier C, Descombes P, François P.** 2011. Orientation and expression of methicillin-resistant Staphylococcus aureus small RNAs by direct multiplexed measurements using the nCounter of NanoString technology. J Microbiol Methods **84:**327–334. http://dx.doi.org/10.1016/j.mimet.2010.12.025.
30. **Beaume M, Hernandez D, Farinelli Deluen LC, Linder P, Gaspin C, Romby P, Schrenzel J, Francois P.** 2010. Cartography of methicillin-resistant *S. aureus* transcripts: detection, orientation and temporal expression during growth phase and stress conditions. PLoS One **5:**e10725. http://dx.doi.org/10.1371/journal.pone.0010725.
31. **Law, CW, Chen Y, Shi W, Smyth GK.** 2014. voom: precision weights unlock linear model analysis tools for RNA-seq read counts. Genome Biol **15:**R29. http://dx.doi.org/10.1186/gb-2014-15-2-r29.
32. **Ritchie ME, Phipson B, Wu D, Hu Y, Law CW, Shi W, Smyth GK.** 2015. limma powers differential expression analyses for RNA-sequencing and microarray studies. Nucleic Acids Res **43:**e47. http://dx.doi.org/10.1093/nar/gkv007.
33. **Posada AC, Kolar SL, Dusi RG, Francois P, Roberts AA, Hamilton CJ, Liu GY, Cheung A.** 2014. Importance of bacillithiol in the oxidative stress response of *Staphylococcus aureus*. Infect Immun **82:**316–332. http://dx.doi.org/10.1128/IAI.01074-13.
34. **Cordin O, Banroques J, Tanner NK, Linder P.** 2006. The DEAD-box protein family of RNA helicases. Gene **367:**17–37. http://dx.doi.org/10.1016/j.gene.2005.10.019.
35. **Hunger K, Beckering CL, Wiegeshoff F, Graumann PL, Marahiel MA.** 2006. Cold-induced putative DEAD box RNA helicases CshA and CshB are essential for cold adaptation and interact with cold shock protein B in *Bacillus subtilis*. J Bacteriol **188:**240–248. http://dx.doi.org/10.1128/JB.188.1.240-248.2006.
36. **Oun S, Redder P, Didier JP, François P, Corvaglia AR, Buttazzoni E, Giraud C, Girard M, Schrenzel J, Linder P.** 2013. The CshA DEAD-box RNA helicase is important for quorum sensing control in *Staphylococcus aureus*. RNA Biol **10:**157–165. http://dx.doi.org/10.4161/rna.22899.
37. **Linder P, Lasko PF, Ashburner M, Leroy P, Nielsen PJ, Nishi K, Schnier J, Slonimski PP.** 1989. Birth of the D-E-A-D box. Nature **337:**121–122. http://dx.doi.org/10.1038/337121a0.
38. **Yoneyama M, Kikuchi M, Natsukawa T, Shinobu N, Imaizumi T, Miyagishi M, Taira K, Akira S, Fujita T.** 2004. The RNA helicase RIG-I has an essential function in double-stranded RNA-induced innate antiviral responses. Nat Immunol **5:**730–737. http://dx.doi.org/10.1038/ni1087.
39. **Warrener P, Collett MS.** 1995. Pestivirus NS3 (p80) protein possesses RNA helicase activity. J Virol **69:**1720–1726.
40. **Bohn C, Rigoulay C, Bouloc P.** 2007. No detectable effect of RNA-binding protein Hfq absence in *Staphylococcus aureus*. BMC Microbiol **7:**10. http://dx.doi.org/10.1186/1471-2180-7-10.
41. **Tanner NK, Cordin O, Banroques J, Doère M, Linder P.** 2003. The Q motif. A newly identified motif in DEAD box helicases may regulate ATP binding and hydrolysis. Mol Cell **11:**127–138.
42. **Iost I, Dreyfus M.** 2006. DEAD-box RNA helicases in *Escherichia coli*. Nucleic Acids Res **34:**4189–4197. http://dx.doi.org/10.1093/nar/gkl500.
43. **Giraud C, Hausmann S, Lemeille S, Prados J, Redder P, Linder P.** 2015. The C-terminal region of the RNA helicase CshA is required for the interaction with the degradosome and turnover of bulk RNA in the opportunistic pathogen *Staphylococcus aureus*. RNA Biol **12:**658–674. http://dx.doi.org/10.1080/15476286.2015.1035505.
44. **Lehnik-Habrink M, Pförtner H, Rempeters L, Pietack N, Herzberg C, Stülke J.** 2010. The RNA degradosome in *Bacillus subtilis*: identification of CshA as the major RNA helicase in the multiprotein complex. Mol Microbiol **77:**958–971. http://dx.doi.org/10.1111/j.1365-2958.2010.07264.x.
45. **Roux CM, DeMuth JP, Dunman PM.** 2011. Characterization of components of the *Staphylococcus aureus* mRNA degradosome holoenzyme-like complex. J Bacteriol **193:**5520–5526. http://dx.doi.org/10.1128/JB.05485-11.
46. **Gottesman S, Storz G.** 2011. Bacterial small RNA regulators: versatile roles and rapidly evolving variations. Cold Spring Harb Perspect Biol **3:**a003798. http://dx.doi.org/10.1101/cshperspect.a003798.
47. **Stead MB, Marshburn S, Mohanty BK, Mitra J, Castillo LP, Ray D, van Bakel H, Hughes TR, Kushner SR.** 2011. Analysis of *Escherichia coli* RNase E and RNase III activity *in vivo* using tiling microarrays. Nucleic Acids Res **39:**3188–3203. http://dx.doi.org/10.1093/nar/gkq1242.
48. **Romilly C, Caldelari I, Parmentier D, Lioliou E, Romby P, Fechter P.** 2012. Current knowledge on regulatory RNAs and their machineries in *Staphylococcus aureus*. RNA Biol **9:**402–413. http://dx.doi.org/10.4161/rna.20103.
49. **Geisinger E, Adhikari RP, Jin R, Ross HF, Novick RP.** 2006. Inhibition of *rot* translation by RNAIII, a key feature of *agr* function. Mol Microbiol **61:**1038–1048. http://dx.doi.org/10.1111/j.1365-2958.2006.05292.x.
50. **Lioliou E, Sharma CM, Caldelari I, Helfer A, Fechter P, Vandenesch F, Vogel J, Romby P.** 2012. Global regulatory functions of the *Staphylococcus aureus* endoribonuclease III in gene expression. PLoS Genet **8:**e1002782. http://dx.doi.org/10.1371/journal.pgen.1002782.
51. **Arnaud M, Chastanet A, Débarbouillé M.** 2004. New vector for efficient allelic replacement in naturally nontransformable, low-GC-content, Gram-positive bacteria. Appl Environ Microbiol **70:**6887–6891. http://dx.doi.org/10.1128/AEM.70.11.6887-6891.2004.
52. **Silverman E, Edwalds-Gilbert G, Lin RJ.** 2003. DExD/H-box proteins and their partners: helping RNA helicases unwind. Gene **312:**1–16. http://dx.doi.org/10.1016/S0378-1119(03)00626-7.